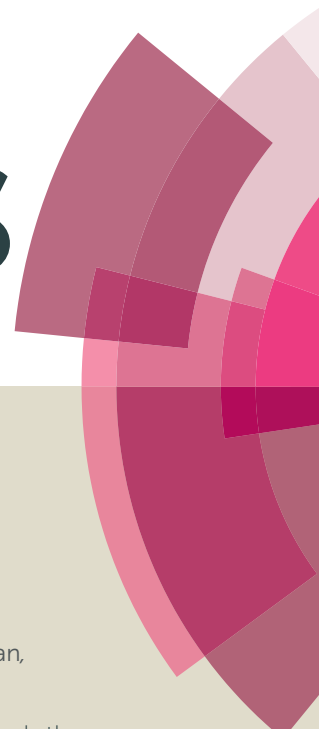


RSC Advances



This article can be cited before page numbers have been issued, to do this please use: S. M. Baghbanian, *RSC Adv.*, 2014, DOI: 10.1039/C4RA10537K.



This is an *Accepted Manuscript*, which has been through the Royal Society of Chemistry peer review process and has been accepted for publication.

Accepted Manuscripts are published online shortly after acceptance, before technical editing, formatting and proof reading. Using this free service, authors can make their results available to the community, in citable form, before we publish the edited article. This *Accepted Manuscript* will be replaced by the edited, formatted and paginated article as soon as this is available.

You can find more information about *Accepted Manuscripts* in the [Information for Authors](#).

Please note that technical editing may introduce minor changes to the text and/or graphics, which may alter content. The journal's standard [Terms & Conditions](#) and the [Ethical guidelines](#) still apply. In no event shall the Royal Society of Chemistry be held responsible for any errors or omissions in this *Accepted Manuscript* or any consequences arising from the use of any information it contains.

Cite this: DOI: 10.1039/c0xx00000x

www.rsc.org/xxxxxx

ARTICLE TYPE

Synthesis, characterization and application of Cu₂O and NiO nanoparticles supported onto natural nanozeolite clinoptilolite as heterogeneous catalyst for the synthesis of pyrano[3,2-*b*]pyrans and pyrano[3,2-*c*]pyridones

Seyed Meysam Baghbanian*

Received (in XXX, XXX) Xth XXXXXXXXXX 20XX, Accepted Xth XXXXXXXXXX 20XX

DOI: 10.1039/b000000x

In this research, the synthesis of Cu₂O and NiO nanoparticles supported onto natural nanozeolite Clinoptilolite (CP) were found to be a recoverable catalyst system for the synthesis of pyrano-[3,2-*c*]pyridone and pyrano[3,2-*b*]pyran derivatives in aqueous media. The nanocatalysts were characterized by various techniques such as XRD, BET, SEM, TEM, TEM-EDS and XPS analyses. TEM study reveals that Cu₂O and NiO nanoparticles have particle size less than 10 nm. XRD and XPS characterizations show that the existence forms of Cu₂O or NiO on the surface of natural nanozeolite CP. The easy recovery of the catalyst and high yield of the products make the protocol attractive and economic. Furthermore, the nanocatalysts could be recycled and reused several times without significant loss of their catalytic activities.

1. Introduction

Zeolite Clinoptilolite (CP) is microporous aluminosilicates that are [SiO₄]⁴⁻ and [AlO₄]⁴⁻ tetrahedral that link together to form a three dimensional structure of well-defined pores and channels, a negative charge is associated with each Al atom. The general formula for the composition of CP is M_{x/n}[(AlO₂)_x(SiO₂)_y]·mH₂O where M is represents cations of n valence that balance the negative charges on the framework. The aluminium in the zeolite framework has a substantial negative charge that is balanced by exchangeable cations such as Na⁺ or K⁺. These cations can be easily exchanged by simply stirring the zeolite in an aqueous solution containing the desired cation that due to their unique properties, CP can be employed as catalyst for the synthesis of organic compounds.¹ Therefore, the investigation on the use of "CP" as a reliable catalyst support seems to be worth mentioning. So, we considered the applicability of this valuable multipurpose compound as a support of metal catalyst due to its great characteristics including high and adjustable acidity, well defined pore structures with channels and cavities of molecular dimensions and high ion exchange capabilities.²

Pyranopyridone derivatives have been found to possess a wide spectrum of biological actions such as antibacterial,³ antifungal and antialgal,⁴ anti-inflammatory,⁵ antileishmanial,⁶ platelet aggregation,⁷ and nitric oxide production.⁸ Furthermore, several pyranopyridone including alkaloids exhibit cancer cell growth inhibitory activity and are investigated as potent anticancer agents.⁹ Pyranopyran derivatives also are an important class of structural pattern of many natural and synthetic compounds which have a high activity profile due to their wide range of biological activities such as anticancer,¹⁰ anti-tuberculosis,¹¹ anti-HIV,¹² calcium channel antagonist activity,¹³ antifungal,¹⁴ antimicrobial,¹⁵ antiproliferative,¹⁶ antidiabetic,¹⁷ anti-inflammatory and antiviral.¹⁸ On the other hand, pyranopyranones are also known for their biological properties including antioxidant and cytotoxic activities.¹⁹ Therefore, the synthesis of pyrano-[3,2-*c*]pyridone and pyrano[3,2-*b*]pyran skeletons are of enormous importance in organic synthesis.

In recent years, efficient methods have been developed for the synthesis of pyrano-[3,2-*c*]pyridone and pyrano[3,2-*b*]pyran derivatives with the aim of preparing of a new series of a fused heterocyclic systems exhibiting high levels of biological activity using a range of different catalysts.^{3-18,20} Although these methods are effective, but most of them still have some drawbacks resulting in significant limits on their synthetic applications such as most of the catalyst are synthetic and require laborious, time-consuming, high reaction temperatures, use of toxic solvents and moderate yields. Thus, development of a simple, eco-benign, low cost protocol, using neutral and reusable catalyst for one-pot synthesis of pyrano-[3,2-*c*]pyridone and

*Department of Chemistry, Ayatollah Amoli Branch, Islamic Azad University, P.O. Box 678, Amol, Iran;

E-mail: S.M.Baghbanian@iautamol.ac.ir†Electronic Supplementary Information Electronic supplementary information (ESI) available: See DOI: 10.1039/b000000x

pyrano[3,2-*b*]pyran derivatives still remains as an attractive goal for researchers. In this work, in continuation of our investigations into the development of new catalysts,²¹ we describe here synthesis, characterization and application of Cu₂O and NiO nanoparticles supported onto nanozeolite CP as a heterogeneous catalyst in the synthesis of pyrano-[3,2-*c*]pyridone and pyrano[3,2-*b*]pyran derivatives in aqueous media.

2. Results and discussion

The nanozeolite CP was prepared according to a simple method developed recently by our group.^{21a} Initially the nanozeolite clinoptilolite was converted to the homoionic Na⁺-exchanged form by stirring in 2 M NaCl solution and subsequently activated with 4 M sulfuric acid. The activated nanozeolite CP was designated as AT-Nano CP. AT-Nano CP was taken into a round bottom flask and an aqueous solution of MCl₂ (M= Cu and Ni) was added under vigorous stirring condition to afforded Cu and Ni exchanged AT-nano CP. Finally, the M-containing products were carried out by heating under air to give Cu₂O and NiO nanoparticles into pores of AT-Nano CP. The nano catalysts were characterized by XRD, BET, SEM, TEM, TEM-EDS and XPS.

XRD pattern of AT-Nano CP (Fig. 1a) shows peaks at $2\theta = 22.0^\circ$, 27.96° and 35.92° which agrees with the natural zeolite of clinoptilolite (JCPDS 00-025-1349). This revealed that the surface modification of AT-Nano CP do not lead to their phase change. X-ray diffraction of nano Cu₂O-CP (Fig. 1b) contains the above peaks together with an obvious diffusion peak at 42.4° , 62.5° and 73.6° could be corresponding to the (200), (220) and (311) planes of Cu₂O crystal with a cubic phase (JCDs 78–2076) and the pattern of nano NiO-CP (Fig. 1c) also consist of two characteristic diffraction peaks appear at 45.4° and 63.5° , which correspond to the (200) and (220) planes of NiO crystal with a cubic phase (JCPDS, No. 71-1179). These new peaks, observed in the XRD patterns of nano Cu₂O-CP and NiO-CP may be due to encapsulation of nano Cu₂O or NiO in the cavity of nanozeolite CP. Further, a little change occurred in the relative peak intensities of nanozeolite upon introducing nano Cu₂O-CP or nano NiO-CP. These observations indicate that the crystallinity of the nanozeolite has not undergone any significant change during the process of encapsulation. The average crystallite size for nano Cu₂O and nano NiO were calculated based on the strongest intensity of (220) peak using the Debye-Scherrer's formula $D = 0.89\lambda/(\beta\cos\theta)$; where D is the grain size, β is the angular line width of half-maximum intensity in radians, θ is Bragg diffraction angle and λ is the X-ray wavelength used. The average size is found to be below 10 nm.

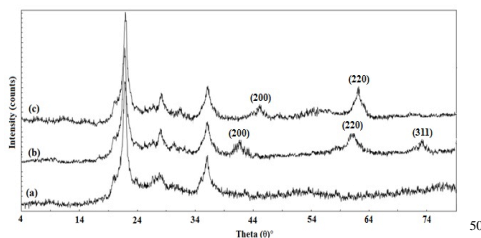


Fig. 1. XRD patterns of (a) AT-Nano CP, (b) nano Cu₂O-CP and (c) nano NiO-CP

The N₂ adsorption-desorption isotherms for nano CP, AT-Nano CP, nano Cu₂O-CP and nano NiO-CP were measured and the specific surface area (*S*), the total pore and micropore volumes (*V*_{tot} and *V*_{mic}), the specific surface area (*S*_{BET}) and the average pore diameter (*D*) were calculated using the Brunauer-Emmett-Teller (BET) method (supporting information). Using the Barrett-Joyner-Halenda (BJH) method, the mesopore surface area *S*_{BJH} and the mesopore volume *V*_{BJH} were calculated for nano CP, AT-Nano CP, nano Cu₂O-CP and nano NiO-CP and summarized in Table 1. According to the Brunauer, Deming, Dering and Teller (BDDT) classification, characteristic of mesoporous solids,²² All the materials displayed typical type IV with an H₃ hysteresis loop at *P/P*₀ ~ 0.984. The nano CP with average pore diameters ~12.20 nm contained a specific surface area of 49.7 m².g⁻¹ and a specific pore volume of 0.15 cm³.g⁻¹. Increase in the specific surface area from 49.7 m².g⁻¹ to 55.6 m².g⁻¹ and a slight decrease in the specific pore volume from 0.15 cm³.g⁻¹ to 0.11 cm³.g⁻¹ are observed after the activation of nano CP might be due to the leaching of Al from sites of the zeolite matrix and decationation during acid activation. The BJH curves of nitrogen desorption display descent distribution of pore volume in the mesoporous section (1-100 nm). The pore diameter from 1.64 nm to 1.21 nm and the pore volume from 0.15 cm³.g⁻¹ to 0.11 cm³.g⁻¹ decreased after the activation of nano CP. According to the analysis of the data listed in Table 1, the specific surface area and pore volume were decreased after encapsulation of nano Cu₂O or NiO in the cavity of AT-Nano CP can be due to clogging of some pores by nano Cu₂O or NiO. Since that a sudden change has not occurred in the specific pore volume and surface area of AT-Nano CP upon introducing nano Cu₂O-CP or nano NiO-CP further approves that pores of AT-Nano CP are not clogged by nano Cu₂O-CP or nano NiO-CP larger than the pore size of AT-Nano CP. Accordingly, from the obtained results one could just conclude that nano Cu₂O-CP or nano NiO-CP were grafted on the pores of AT-Nano CP.

Table 1. Surface properties of different nanozeolite based support/catalysts

Sample	Specific surface area [m ² .g ⁻¹]		Pore volume [cm ³ .g ⁻¹]		Pore diameter [nm]	
	<i>S</i> _{BET}	<i>S</i> _{BJH}	<i>V</i> _{tot} (BET)	<i>V</i> (BJH)	<i>D</i> _{av}	<i>D</i> (BJH)
Nano CP	49.70	45.68	0.15	0.15	12.19	1.64
AT-Nano CP	55.63	39.52	0.11	0.1	8.05	1.21
Nano Cu ₂ O-CP	47.4	38.41	0.09	0.11	10.07	1.63
Nano NiO-CP	49.1	35.47	0.08	0.12	8.88	1.26

The structural and morphological characterization of nano CP, AT-Nano CP, nano Cu₂O-CP and nano NiO-CP were performed using SEM (Fig. 3). Comparison of the SEM images of nano CP (Fig. 3a), AT-Nano CP (Fig. 3b), nano Cu₂O-CP (Fig. 3c) and nano NiO-CP (Fig. 3d) shows that the morphological features are not changed significantly such as the spherical or ellipsoidal shape and non-aggregation characteristics. SEM image of nano Cu₂O-CP and nano NiO-CP also showed that the average particle size was found in the range of 35-85 nm.

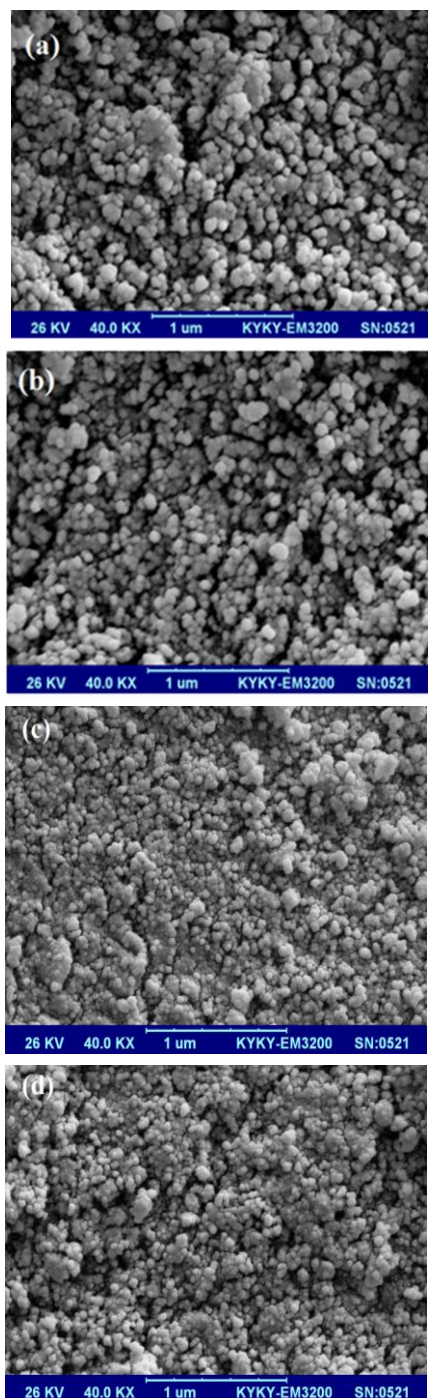


Fig 3. SEM images of (a) Nano CP, (b) AT-Nano CP and (c) Cu_2O -CP and (d) nano NiO-CP

The morphology and size of Cu_2O -CP (Fig. 4a) and nano NiO-CP (Fig. 4b) were investigated by transmission electron microscopy (TEM). The pictures show that the average particle size of Cu_2O and NiO is below 10 nm. As shown in Fig. 4a and b, the anchored crystal Cu_2O and NiO nanoparticles distributed evenly on the nanozeolite CP without obvious aggregations and particles can deposit on the pores of these nanozeolite. The results from the TEM studies are in general in agreement with the results obtained from X-ray diffraction measurements. The Cu_2O and NiO nanoparticles deposition on the AT-Nano CP was further

confirmed by energy-dispersive X-ray spectroscopy on a TEM (TEM-EDS). The results reveal presence of C, O, Al, Si and Cu in nano Cu_2O -CP (Fig. 4c) and C, O, Al, Si and Ni in nano NiO-CP (Fig. 4d).

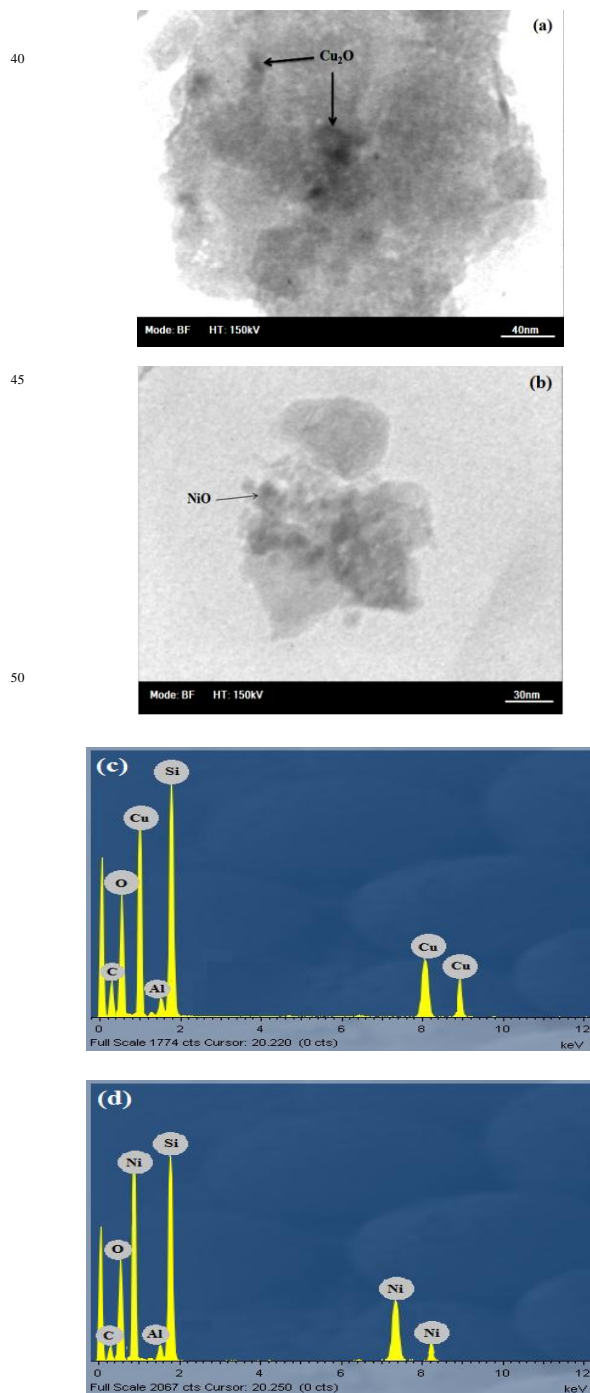


Fig 4. TEM images of (a) Nano Cu_2O -CP and (b) Nano NiO-CP. TEM-EDS data of (c) Nano Cu_2O -CP (d) Nano NiO-CP.

The surface properties of nano Cu_2O -CP and nano NiO-CP were analyzed using XPS. The peaks at 931.9 and 952.3 eV corresponding to $\text{Cu } 2p_{3/2}$ and $\text{Cu } 2p_{1/2}$ are clearly observed in

Fig. 5a. The Cu 2p_{3/2} peak can be assigned to Cu₂O in accordance with data in the literature.²³ Fig. 5b shows the core level spectra for the Ni 2p peak over the binding energy ranges from 850-885 eV. The Ni 2p XPS spectrum shows two edges of Ni 2p_{3/2} (from about 855 eV to 865 eV) and Ni 2p_{1/2} (from about 868 eV to 885 eV), which confirms the presence of the corresponding elements for the NiO nano metal shell. The Ni 2p_{1/2} (872.1 eV) and Ni 2p_{3/2} (854.3 eV) peaks were assigned to the Ni(II) ions in NiO.²⁴ The splitting separation between these two main peaks, namely, 17.8 eV, indicated the well-defined symmetry of Ni(II) ion in oxide form.

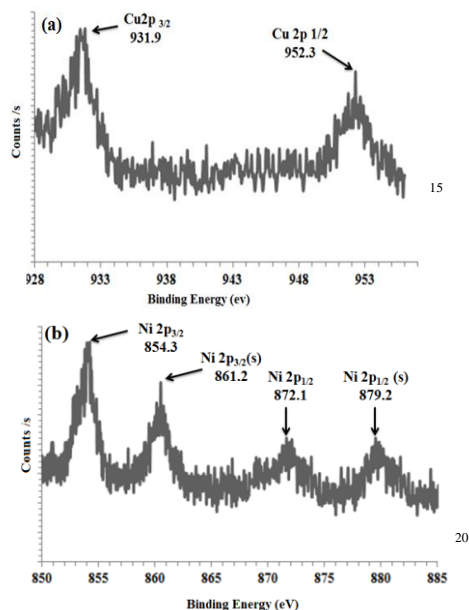
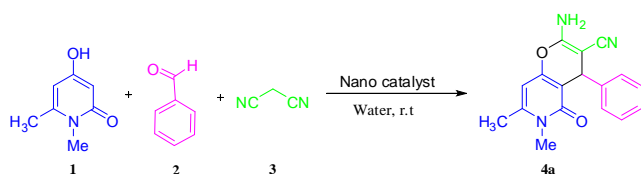


Fig. 5. XPS spectrum of (a) Cu 2p spectral peaks of Nano Cu₂O-CP and (b) Ni 2p spectral peaks of Nano NiO-CP

These nanocatalysts were then explored as a heterogeneous catalyst for the synthesis of pyrano-[3,2-*c*]pyridones and pyrano[3,2-*b*]pyrans derivatives via three-component reaction. In order to find the best reaction conditions for the synthesis of pyrano-[3,2-*c*]pyridones, the reaction of 4-hydroxy-1,6-dimethylpyridin-2(1*H*)-one **1** (1 mmol) with benzaldehyde **2** (1 mmol) and malononitrile **3** (1 mmol) was chosen as a model reaction in water at room temperature (Scheme 1).



Scheme 1 The model reaction for the synthesis of pyrano-[3,2-*c*]pyridone **4a**

The reaction was carried out in the presence of nano Cu₂O-CP, nano NiO-CP, AT-Nano CP, CuO and NiO nanoparticles, and the results are presented in Table 2. In the absence of catalyst, only a trace amount of desired product was obtained even after longer

40 reaction time (Table 2, entry 1). The results show that all of nano catalysts could promote the reaction, but nano Cu₂O-CP catalyst is significantly more effective than other catalysts in the synthesis of pyrano-[3,2-*c*]pyridone **4a** and it provides better results with high yields.

Table 2. Optimization of reaction conditions for the synthesis of pyrano-[3,2-*c*]pyridone **4a**^a

Entry	Solvent	Catalyst	Amount of the catalyst [g]	Yield [%] ^b
1	H ₂ O	-	-	trace ^c
2	H ₂ O	Nano NiO	0.01	40
3	H ₂ O	Nano Cu ₂ O	0.01	55
4	H ₂ O	AT-Nano CP	0.01	70
5	H ₂ O	Nano NiO-CP	0.004	50
6	H ₂ O	Nano NiO-CP	0.008	65
7	H ₂ O	Nano NiO-CP	0.01	80
8	H ₂ O	Nano Cu ₂ O-CP	0.004	65
9	H ₂ O	Nano Cu ₂ O-CP	0.008	88
10	H₂O	Nano Cu₂O-CP	0.01	92
11	H ₂ O	Nano Cu ₂ O-CP	0.02	92
12	EtOH	Nano Cu ₂ O-CP	0.01	85
13	DMF	Nano Cu ₂ O-CP	0.01	65
14	Toluene	Nano Cu ₂ O-CP	0.01	45
15	CH ₂ Cl ₂	Nano Cu ₂ O-CP	0.01	50

^a Reaction conditions: benzaldehyde (1 mmol), malononitrile (1 mmol), 4-hydroxy-1,6-dimethylpyridin-2(1*H*)-one (1 mmol) and solvent (5 mL) after 1h at room temperature. ^b Isolated yields. ^c After 2h at room temperature

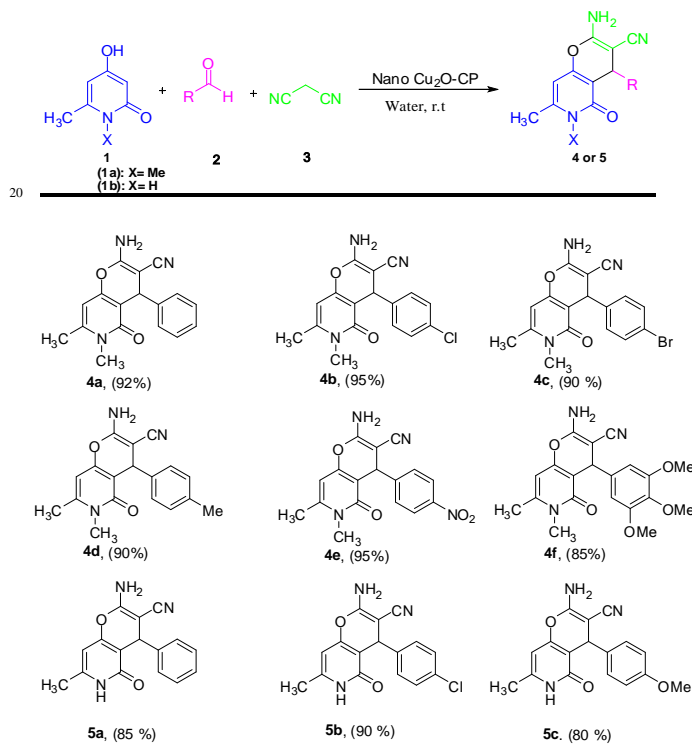
In order to optimize the reaction conditions, the catalytic efficiency was studied with various amounts of nano Cu₂O-CP in the model reaction (Table 2, entries 8-10). The results reveal that 50 0.01 g of nanocatalyst provided the best effects in terms of economy of catalyst charge and purity of products (Table 2, entry 10). Moreover, higher amounts of the catalyst (0.02 gr) did not improve the yield and the reaction time (Table 2, entry 11). The model reaction was also performed in other solvents such as 60 EtOH, DMF, toluene, CH₂Cl₂ and instead of H₂O (Table 2, entries 12-15). Changing the solvent showed no further increase in the yield under optimized conditions. Therefore, the best results were obtained from the reaction of these components in water (5 mL) in the presence of 0.01 g of Nano Cu₂O-CP at room 65 temperature affording the pyrano-[3,2-*c*]pyridone **4a** in a 92% yield (Table 2, entry 10).

The acid strength and acid distribution of AT-nano CP, Nano Cu₂O-CP and Nano NiO-CP measured by amine titration method 70 (n-butylamine titration) using Hammett indicators are listed in Table 3. The limits of the H₀ of samples were recognized by observing the colour of the adsorbed form of the Hammett indicators. The total acid amount for AT-nano CP, Nano Cu₂O-CP and NiO-CP were obtained 2.4, 2.9 and 2.7 mmol/g, 75 respectively. Measurements of surface acidity by amine titration method showed the increase number of Lewis acid sites by the presence of Cu₂O and NiO. These results can explain better performance of Nano Cu₂O-CP than other mesoporous materials in the synthesis of pyrano-[3,2-*c*]pyridone **4a** (Table 2, entries 4- 80 10). Higher activity of Nano Cu₂O-CP compared with alone AT-nano CP and Nano NiO-CP was explained by presence of stronger acid sites connected to zeolite.

Table 3 Acid distribution of AT-nano CP, Cu₂O-CP and NiO-CP catalysts

Catalyst	Acid amount (mmol/g)				Total
	H ₀ ≤ +2.8	H ₀ ≤ +3.3	H ₀ ≤ +4.8	H ₀ ≤ +6.8	
AT-Nano CP	0.9	0	0.7	0.8	2.4
Nano Cu ₂ O-CP	0.9	0.2	0.9	0.9	2.9
Nano NiO-CP	0.9	0.1	0.8	0.9	2.7

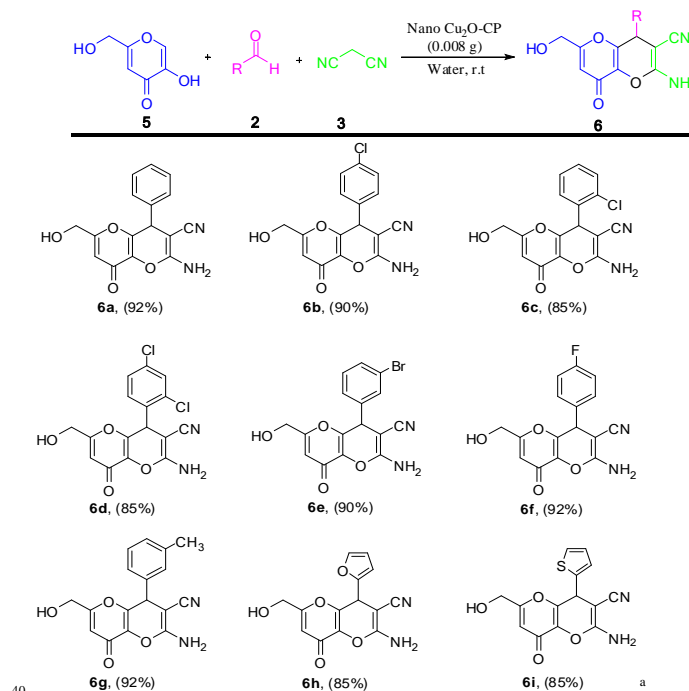
Encouraged by the remarkable results, and in order to show generality and scope of this new protocol, a variety of pyrano[3,2-*c*]pyridone derivatives were synthesized from the three-component reaction of pyridin-2-ones **1a** or **1b** (1 mmol), aromatic aldehydes **2** (1 mmol), and malononitrile **3** (1 mmol) in the presence of nano Cu₂O-CP (0.01 gr) in aqueous medium at room temperature. The results have been summarized in Table 4. According to the results, the substrates with electron-withdrawing groups gave better yields than with electron-donating groups. To develop this reaction into a more general method, other pyridin-2-one substrates, 4-hydroxy-6-methylpyridin-2(1*H*)-one **1b** were also tried (Table 4). They all gave the corresponding products in good to excellent yields.

Table 4 Synthesis of pyrano[3,2-*c*]pyridones **4** and **5** catalyzed by Nano Cu₂O-CP^a

^a Reaction conditions: pyridin-2-ones **1a** or **1b** (1 mmol), aldehyde **2** (1 mmol), malononitrile **3** (1 mmol), Nano Cu₂O-CP (0.01 gr) in 5 mL of water for 1h at room temperature.

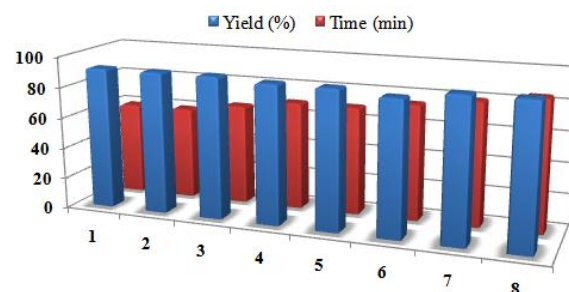
In following to further explore the potential of this protocol, we also examined three component reactions using another reactant, kojic acid **5** instead of pyridin-2-ones **1a,b** under similar reaction conditions (Table 5). Under these conditions, a variety of substituted aromatic aldehydes were applied for the synthesis of pyrano[3,2-*b*]pyran derivatives using of nano Cu₂O-CP under the

optimal reaction conditions and the results are summarized in Table 5. Results demonstrate that all substituted benzaldehydes containing electron-donating or electron-withdrawing substituents in the aromatic ring were reacted with malononitrile to provide the corresponding products **6** in good to excellent yields under optimized reaction conditions.

Table 5 Synthesis of pyrano[3,2-*b*]pyrans **6** catalyzed by Nano Cu₂O-CP^a

Reaction conditions: kojic acid **5** (1 mmol), aromatic aldehydes **2** (1 mmol), malononitrile **3** (1 mmol), Nano Cu₂O-CP (0.01 gr) in 5 mL of water for 1h at room temperature.

The recyclability of the catalyst for reactions was investigated. The catalyst was recovered by filtration technique after each experiment and washed with hot distilled water (2 mL) and ethanol (2 mL) twice. The recovered catalyst was dried in an oven and reused successively several times (up to 8 uses) without any significant loss of activity (Fig. 6). The strong interaction of Cu₂O nanoparticles with the zeolite surface could be the reason for the repetitive use of the catalyst in a greater number of catalytic runs with high efficiency.

**Fig. 6** The reusability of nano Cu₂O-CP separable catalyst

In the present study, a reproducible synthetic procedure has been developed to prepare Cu₂O and NiO nanoparticles into the nanopores of modified nanozeolite clinoptilolite. The presence of nano NiO and Cu₂O in the nanozeolite has a significant influence on the acidity of the clinoptilolite skeleton leading to an increase in the number of Lewis acid sites. The results indicate that nano Cu₂O-CP could be considered as catalyst for the synthesis of pyrano-[3,2-*c*]pyridone and pyrano[3,2-*b*]pyran derivatives in good to excellent yields. These nanocatalysts are thermally stable, inexpensive, and easy to prepare. In addition, it could be easily separated from the reaction mixture and reused for several times without any significant loss of its activity.

4. Experimental Section

4.1. Materials

All reagents were prepared from analytical reagent grade chemicals unless specified otherwise and purchased from Merck Company. The raw zeolite material was an Iranian commercial Clinoptilolite (Afrandtooska Company) obtained from deposits in the region of Semnan (ca. 1 \$ per kg).

4.2. Instrumentation

The X-ray powder diffraction (XRD) of the catalyst was carried out on a Philips PW 1830 X-ray diffractometer with Cu K α source ($\lambda=1.5418 \text{ \AA}$) in a range of Bragg's angle (10-90°) at room temperature. N₂ sorption measurement was performed using Belsorp mini II at 273 K. Prior to the measurements, all the samples were degassed at 393 K in a vacuum line overnight. The specific surface area and pore volume were calculated with the Brunauer-Emmett-Teller (BET) method, and the pore size distribution was expected with desorption branch based on the Barrett-Joyneer-Halenda (BJH) model. Scanning electron microscope (SEM) pictures were taken using KYKY-EM3200 microscope (acceleration voltage 26 kV). Transmission electron microscopy (TEM) experiments were conducted on a JEOL-2100 microscope operated at 150 KV. The TEM model Samples are sonicated by mixing with 95% ethanol for 30 min, and subsequently dropped onto copper grids coated with carbon film, and dried thoroughly in an electronic drying cabinet at a temperature of 25 °C and relative humidity 45%. The chemical composition and crystallinity analysis of the samples are characterized using an energy-dispersive X-ray spectrometer (EDS, INCA) operated at 150 KV. X-ray photoelectron spectra (XPS) were recorded on a BESTEC GmbH-8025 spectrometer using an Mg K α (hv = 1253.6 eV) and Al K α (hv = 1486.6 eV) X-ray source. ¹H, ¹³C NMR spectra were recorded on a BRUKER DRX-400 AVANCE spectrometer.

4.3. Catalyst preparation

4.3.1. Preparation of AT-Nano CP

The nanozeolite clinoptilolite was converted to the homoionic Na⁺-exchanged form by stirring in 2 mol L⁻¹ of NaCl solution for about 24 h at 25 °C, and then the Na⁺-nanozeolite clinoptilolite was filtrated and washed with distilled water (50 mL) two times. The Na⁺-nanozeolite was dried in an oven at 100 °C. The Na⁺-nanozeolite clinoptilolite (5 g) was taken into a 250 mL round bottom flask and 100 mL 4 M sulfuric acid was added to it. The

flask mixture was refluxed for 1 h. After cooling, the supernatant was discarded and the activated nanozeolite clinoptilolite was repeatedly washed with deionized water (250 mL) until the solution became neutral and finally dried in oven at 80 °C overnight to obtain the white solid product. The activated nanozeolite clinoptilolite was designated as AT-Nano CP.

4.3.2. Preparation of Cu and Ni oxide nanoparticles on the surface of AT-Nano CP

One gram of AT-Nano CP was taken into a 100 mL round bottom flask and 100 cm³ of 25 mmol L⁻¹ MCl₂ (M= Cu and Ni) was added slowly under vigorous stirring condition. The resulting mixture was stirred for 24 h at room temperature, and the M-containing product was then recovered by filtration. The suspension was filtered off, washed with water and dried at 80 °C. Dehydration of the M-containing products was carried out by heating under air. The obtained Cu and Ni exchanged AT-nano CP were heated at a heating rate of 10 °C min⁻¹ to 550 °C and then were isothermally heated for 60 min. The influence of Cu₂O and NiO loading on AT-Nano CP was studied using the same experimental conditions. According to atomic absorption results of copper and nickel determination, their Cu₂O and NiO contents were 200 and 95 mg Cu₂O and NiO per gram of the catalyst, respectively.

4.3.3. General procedure for the synthesis of pyrano-[3,2-*c*]pyridone and pyrano[3,2-*b*]pyran derivatives

A mixture of 4-hydroxy-1,6-dimethylpyridin-2(1*H*)-one or 5-hydroxy-2-(hydroxymethyl)-4*H*-pyran-4-one or 4-hydroxy-6-methylpyridin-2(1*H*)-one (1 mmol), aldehyde (1 mmol), malononitrile (1 mmol), and catalyst (0.01 g) in 5 mL of water was stirred at room temperature for 1 h (Table 3 and 4). After this time, the catalyst was removed by filtration, washed with ethanol (2 mL), dried in vacuum and reused. The filtrate was evaporated under reduced pressure to give the desired product and recrystallized from hot ethanol to afford pure products. The products were characterized by ¹H and ¹³C NMR.

4.4. Spectral data of the synthesized compounds

4.4.1. 2-Amino-5,6-dihydro-6,7-dimethyl-5-oxo-4-phenyl-4*H*-pyrano[3,2-*c*]pyridine-3-carbonitrile (4a). Mp 250-252 °C. ¹H NMR (400 MHz, DMSO-*d*₆) δ : 2.38 (s, 3H, CH₃), 3.35 (s, 3H, CH₃), 4.42 (s, 1H, CH), 6.12 (s, 1H, CH), 7.09 (s, 2H, NH₂), 7.15-7.21 (m, 3H, ArH), 7.27-7.30 (m, 2H, ArH). ¹³C NMR (100 MHz, DMSO-*d*₆) δ : 21.6, 31.3, 37.5, 58.2, 98.2, 105.0, 120.1, 125.1, 128.2, 128.9, 146.3, 149.5, 155.2, 160.4, 162.7.

4.4.2. 2-Amino-4-(4-chlorophenyl)-5,6-dihydro-6,7-dimethyl-5-oxo-4*H*-pyrano[3,2-*c*]pyridine-3-carbonitrile (4b). Mp 253-256 °C. ¹H NMR (400 MHz, DMSO-*d*₆) δ : 2.35 (s, 3H, CH₃), 3.31 (s, 3H, CH₃), 4.32 (s, 1H, CH), 6.02 (s, 1H, CH), 7.03 (s, 2H, NH₂), 7.14 (d, 2H, *J* = 8.3 Hz, ArH), 7.35 (d, 2H, *J* = 8.3 Hz, ArH). ¹³C NMR (100 MHz, DMSO-*d*₆) δ : 21.1, 31.3, 37.4, 57.8, 98.2, 105.5, 120.4, 128.8, 129.5, 131.4, 144.3, 148.4, 155.1, 160.4, 161.4.

4.4.3. 2-Amino-4-(4-bromophenyl)-5,6-dihydro-6,7-dimethyl-5-oxo-4*H*-pyrano[3,2-*c*]pyridine-3-carbonitrile (4c). Mp 256-257 °C. ¹H NMR (400 MHz, DMSO-*d*₆) δ : 2.33 (s, 3H, CH₃), 3.32 (s, 3H, CH₃), 4.35 (s, 1H, CH), 6.09 (s, 1H, CH), 7.09 (s, 2H, NH₂), 7.15 (d, 2H, *J* = 8.3 Hz, ArH), 7.49 (d, 2H, *J* = 8.3 Hz, ArH). ¹³C

NMR (100 MHz, DMSO- d_6) δ : 21.5, 30.9, 37.2, 57.4, 97.2, 105.3, 119.9, 120.1, 130.6, 132.4, 144.5, 148.4, 155.2, 159.6, 161.8.

4.4.4. 2-Amino-4-(4-methylphenyl)-5,6-dihydro-6,7-dimethyl-5-oxo-4H-pyrano[3,2-c]pyridine-3-carbonitrile (4d). Mp 250-253 °C. ^1H NMR (400 MHz, DMSO- d_6) δ : 2.20 (s, 3H, CH₃), 2.35 (s, 3H, CH₃), 3.33 (s, 3H, CH₃), 4.34 (s, 1H, CH), 6.07 (s, 1H, CH), 6.98 (s, 2H, NH₂), 7.05 (d, 2H, J = 8.3 Hz, ArH), 7.12 (d, 2H, J = 8.3 Hz, ArH). ^{13}C NMR (100 MHz, DMSO- d_6) δ : 21.6, 22.2, 30.7, 37.1, 58.4, 97.3, 106.1, 120.5, 128.1, 129.3, 136.2, 142.3, 147.8, 156.0, 159.4, 161.2.

4.4.5. 2-Amino-5,6-dihydro-6,7-dimethyl-4-(4-nitrophenyl)-5-oxo-4H-pyrano[3,2-c]pyridine-3-carbonitrile (4e). Mp 242-244 °C. ^1H NMR (400 MHz, DMSO- d_6) δ : 2.37 (s, 3H, CH₃), 3.35 (s, 3H, CH₃), 4.58 (s, 1H, CH), 6.12 (s, 1H, CH), 7.13 (br s, 2H, NH₂), 7.52 (d, 2H, J = 8.6 Hz, ArH), 8.20 (d, 2H, J = 8.6 Hz, ArH); ^{13}C NMR (100 MHz, DMSO- d_6) δ : 21.2, 31.2, 37.5, 57.3, 97.6, 105.2, 120.6, 124.5, 130.2, 147.6, 149.2, 152.2, 156.3, 159.5, 161.7.

4.4.6. 2-Amino-6,7-dimethyl-5-oxo-4-(3,4,5-trimethoxyphenyl)-5,6-dihydro-4H-pyrano[3,2-c]pyridine-3-carbonitrile (4f). Mp 259-262 °C. ^1H NMR (400 MHz, DMSO- d_6) δ : 2.32 (s, 3H, CH₃), 3.36 (s, 3H), 3.62 (s, 3H, CH₃), 3.73 (s, 6H, 2CH₃), 4.45 (s, 1H, CH), 6.09 (s, 1H, CH), 6.75 (s, 2H, NH₂), 7.05 (s, 2H, ArH); ^{13}C NMR (100 MHz, DMSO- d_6) δ : 21.2, 31.4, 37.5, 56.7, 58.6, 61.3, 97.1, 104.8, 106.5, 121.2, 138.3, 141.2, 148.6, 153.5, 155.8, 159.7, 161.6.

4.4.7. 2-Amino-5,6-dihydro-7-methyl-5-oxo-4-phenyl-4H-pyrano[3,2-c]pyridine-3-carbonitrile (5a). Mp 279-282 °C. ^1H NMR (400 MHz, DMSO- d_6) δ : 2.13 (s, 3H, CH₃), 4.29 (s, 1H, CH), 5.84 (s, 1H, CH), 7.03 (s, 2H, NH₂), 7.16-7.22 (m, 3H, ArH), 7.28-7.32 (m, 2H, ArH), 11.47 (s, 1H, NH). ^{13}C NMR (100 MHz, DMSO- d_6) δ : 19.4, 37.5, 58.2, 96.3, 106.2, 121.4, 127.1, 127.7, 128.5, 145.4, 147.2, 157.4, 159.1, 161.9.

4.4.8. 2-Amino-4-(4-chlorophenyl)-5,6-dihydro-7-methyl-5-oxo-4H-pyrano[3,2-c]pyridine-3-carbonitrile (5b). Mp 245-247 °C. ^1H NMR (400 MHz, DMSO- d_6) δ : 2.16 (s, 3H, CH₃), 4.35 (s, 1H, CH), 5.87 (s, 1H, CH), 7.07 (s, 2H, NH₂), 7.18 (d, 2H, J = 8.3 Hz, ArH), 7.36 (d, 2H, J = 8.3 Hz, ArH), 11.47 (s, 1H, NH). ^{13}C NMR (100 MHz, DMSO- d_6) δ : 18.7, 36.4, 56.4, 96.3, 106.7, 120.4, 129.2, 129.8, 131.7, 144.8, 147.5, 157.3, 159.5, 161.7.

4.4.9. 2-Amino-5,6-dihydro-4-(4-methoxyphenyl)-7-methyl-5-oxo-4H-pyrano[3,2-c]pyridine-3-carbonitrile (5c). Mp 224-225 °C. ^1H NMR (400 MHz, DMSO- d_6) δ : 2.10 (s, 3H, CH₃), 3.75 (s, 3H, CH₃), 4.35 (s, 1H, CH), 5.92 (s, 1H, CH), 6.98 (d, 2H, J = 8.1 Hz, ArH), 7.05 (s, 2H, NH₂), 7.12 (d, 2H, J = 8.1 Hz, ArH), 11.56 (s, 1H, NH). ^{13}C NMR (100 MHz, DMSO- d_6) δ : 18.6, 35.8, 55.5, 58.7, 96.7, 106.9, 114.2, 120.7, 128.7, 137.2, 146.1, 156.8, 158.2, 159.4, 161.9.

4.4.10. 2-Amino-6-(hydroxymethyl)-8-oxo-4-phenyl-4,8-dihydropyrano[3,2-b]pyran-3-carbonitrile (6a). Mp 222-225 °C. ^1H NMR (400 MHz, DMSO- d_6) δ : 4.15 (dd, 1H, J = 16.5, J = 6.3 Hz, CH_{aliph}), 4.26 (dd, 1H, J = 16.5, J = 6.3 Hz, CH_{aliph}), 5.35 (t, 1H, J = 6.3 Hz, OH), 5.65 (s, 1H, CH_{vinyl}), 6.33 (s, 1H, CH_{aliph}), 7.10 (s, 2H, NH₂), 7.27-7.52 (m, 5H, CH_{arom}); ^{13}C NMR (100 MHz, DMSO- d_6) δ : 40.4, 55.8, 57.5, 111.5, 117.2, 119.2, 128.7, 131.0, 132.3, 135.2, 136.5, 148.1, 159.2, 169.4, 169.9, 195.4.

4.4.11. 2-Amino-4-(4-chlorophenyl)-6-(hydroxymethyl)-8-oxo-

4,8-dihydropyrano[3,2-b]pyran-3-carbonitrile (6b). Mp 195-197 °C. ^1H NMR (400 MHz, DMSO- d_6) δ : 4.12 (dd, 1H, J = 16.5 Hz, J = 6.3 Hz, CH_{aliph}), 4.22 (dd, 1H, J = 16.5 Hz, J = 6.3 Hz, CH_{aliph}), 4.65 (s, 1H, CH_{vinyl}), 5.55 (t, 1H, J = 6.3 Hz, OH), 6.32 (s, 1H, CH_{aliph}), 6.77 (s, 2H, NH₂), 7.20 (d, 2H, J = 8.3 Hz, CH_{arom}), 7.33 (d, 2H, J = 8.3 Hz, CH_{arom}); ^{13}C NMR (100 MHz, DMSO- d_6) δ : 40.5, 55.9, 59.7, 111.5, 119.2, 129.1, 129.5, 134.1, 136.8, 139.2, 148.5, 159.9, 169.3, 170.4.

4.4.12. 2-Amino-4-(2-chlorophenyl)-6-(hydroxymethyl)-8-oxo-4,8-dihydropyrano[3,2-b]pyran-3-carbonitrile (6c). Mp 212-215 °C. ^1H NMR (400 MHz, DMSO- d_6) δ : 4.18 (dd, 1H, J = 16.5, J = 6.3 Hz, CH_{aliph}), 4.54 (dd, 1H, J = 16.5, J = 6.3 Hz, CH_{aliph}), 5.21 (t, 1H, J = 6.3 Hz, OH), 5.77 (s, 1H, CH_{vinyl}), 6.39 (s, 1H, CH_{aliph}), 7.09 (s, 2H, NH₂), 7.25-7.59 (m, 4H, CH_{arom}); ^{13}C NMR (100 MHz, DMSO- d_6) δ : 40.1, 54.7, 59.5, 111.5, 118.9, 128.3, 129.8, 130.5, 131.2, 131.9, 136.7, 137.5, 148.3, 159.6, 167.8, 169.2, 196.1.

4.4.13. 2-Amino-4-(2,4-dichlorophenyl)-6-(hydroxymethyl)-8-oxo-4,8-dihydropyrano[3,2-b]pyran-3-carbonitrile (6d). Mp 240-241 °C. ^1H NMR (400 MHz, DMSO- d_6) δ : 4.13 (dd, 1H, J = 16.5, J = 6.3 Hz, CH_{aliph}), 4.32 (dd, 1H, J = 16.5, J = 6.3 Hz, CH_{aliph}), 5.52 (t, 1H, J = 6.3 Hz, OH), 5.89 (s, 1H, CH_{vinyl}), 6.45 (s, 1H, CH_{aliph}), 7.49 (s, 2H, NH₂), 7.50 (d, 1H, J = 8.3 Hz, CH_{arom}), 7.92 (d, 1H, J = 2.5 Hz, CH_{arom}), 7.95 (dd, 1H, J = 8.3, J = 2.5 Hz, CH_{arom}); ^{13}C NMR (100 MHz, DMSO- d_6) δ : 39.7, 55.3, 59.4, 117.5, 119.1, 128.4, 129.4, 129.7, 130.6, 131.9, 136.5, 138.2, 149.1, 159.9, 169.1, 170.2, 192.3.

4.4.14. 2-Amino-4-(3-bromophenyl)-6-(hydroxymethyl)-8-oxo-4,8-dihydropyrano[3,2-b]pyran-3-carbonitrile (6e). Mp 244-245 °C. ^1H NMR (400 MHz, DMSO- d_6) δ : 4.18 (dd, 1H, J = 16.5, J = 6.3 Hz, CH_{aliph}), 4.35 (dd, 1H, J = 16.5, J = 6.3 Hz, CH_{aliph}), 5.78 (t, 1H, J = 6.3 Hz, OH), 5.84 (s, 1H, CH_{vinyl}), 6.73 (s, 1H, CH_{aliph}), 7.24 (s, 2H, NH₂), 7.48-7.83 (m, 4H, CH_{arom}); ^{13}C NMR (100 MHz, DMSO- d_6) δ : 38.9, 55.1, 59.5, 112.9, 119.5, 123.1, 127.1, 131.5, 130.7, 135.6, 137.1, 143.3, 145.4, 159.5, 168.3, 169.6, 195.2.

4.4.15. 2-Amino-4-(4-fluorophenyl)-6-(hydroxymethyl)-8-oxo-4,8-dihydropyrano[3,2-b]pyran-3-carbonitrile (6f). Mp 249-252 °C. ^1H NMR (400 MHz, DMSO- d_6) δ : 4.19 (dd, 1H, J = 16.3, J = 6.0 Hz, CH_{aliph}), 4.33 (dd, 1H, J = 16.3, J = 6.0 Hz, CH_{aliph}), 4.78 (t, 1H, J = 6.0 Hz, OH), 5.69 (s, 1H, CH_{vinyl}), 6.44 (s, 1H, CH_{aliph}), 7.20-7.27 (m, 2H, CH_{arom}), 7.30 (s, 2H, NH₂), 7.35-7.46 (m, 2H, CH_{arom}); ^{13}C NMR (100 MHz, DMSO- d_6) δ : 39.5, 56.5, 59.4, 112.4, 116.5 (d, J = 25.0 Hz, C-F), 119.7, 129.5 (d, J = 9.8 Hz, C-F), 136.5, 137.5 (d, J = 3.8 Hz, C-F), 149.1, 160.2, 162.4 (d, J = 295.2 Hz, C-F), 168.5, 169.7, 198.6.

4.4.16. 2-Amino-6-(hydroxymethyl)-8-oxo-4-m-tolyl-4,8-dihydropyrano[3,2-b]pyran-3-carbonitrile (6g). Mp 221-222 °C. ^1H NMR (400 MHz, DMSO- d_6) δ : 2.38 (s, 3H, CH₃), 4.28 (dd, 1H, J = 16.2, J = 6.2 Hz, CH_{aliph}), 4.26 (dd, 1H, J = 16.2, J = 6.2 Hz, CH_{aliph}), 4.81 (t, 1H, J = 6.2 Hz, OH), 5.72 (s, 1H, CH_{vinyl}), 6.38 (s, 1H, CH_{aliph}), 6.79 (d, 1H, J = 8.0 Hz, CH_{arom}), 7.18 (d, 1H, J = 8.0 Hz, CH_{arom}), 7.12 (s, 2H, NH₂), 7.32 (t, 1H, J = 8.0 Hz, CH_{arom}); ^{13}C NMR (100 MHz, DMSO- d_6) δ : 32.9, 55.5, 59.2, 111.4, 119.6, 125.1, 128.1, 128.8, 137.3, 138.3, 141.1, 149.4, 159.2, 167.4, 169.5, 195.6.

4.4.17. 2-Amino-4-(furan-2-yl)-6-(hydroxymethyl)-8-oxo-4,8-dihydropyrano[3,2-b]pyran-3-carbonitrile (6h). Mp 223-225 °C. ^1H NMR (400 MHz, DMSO- d_6) δ : 4.18 (dd, 1H, J = 16.5, J = 6.3

Hz, CH_{aliph}), 4.27 (dd, 1H, *J* = 16.5, *J* = 6.3 Hz, CH_{aliph}), 4.72 (t, 1H, *J* = 6.3 Hz, OH), 5.24 (s, 1H, CH_{vinyl}), 6.47 (s, 1H, CH_{aliph}), 7.21 (s, 2H, NH₂), 7.47 (d, 2H, *J* = 4.8 Hz, CH_{arom}), 7.56-7.67 (m, 2H, CH_{arom}); ¹³C NMR (100 MHz, DMSO-*d*₆) δ = 34.5, 55.6, 59.3, 107.6, 110.7, 112.1, 112.9, 118.5, 142.1, 142.8, 153.4, 159.5, 169.1, 197.2.

4.4.18. 2-Amino-6-(hydroxymethyl)-8-oxo-4-(thiophen-2-yl)-4,8-dihydropyrano[3,2-*b*]pyran-3-carbonitrile (6i). Mp 233-236 °C. ¹H NMR (400 MHz, DMSO-*d*₆) δ = 4.22 (dd, 1H, *J* = 16.5, *J* = 6.3 Hz, CH_{aliph}), 4.32 (dd, 1H, *J* = 16.5, *J* = 6.3 Hz, CH_{aliph}), 5.14 (t, 1H, *J* = 6.2 Hz, OH), 5.31 (s, 1H, CH_{vinyl}), 6.37 (s, 1H, CH_{aliph}), 7.02 (s, 2H, NH₂), 7.44 (d, 2H, *J* = 5.4, CH_{arom}), 7.52-7.69 (m, 2H, CH_{arom}); ¹³C NMR (100 MHz, DMSO-*d*₆) δ = 37.1, 57.3, 59.3, 111.7, 112.7, 119.7, 124.6, 125.4, 128.3, 140.2, 143.2, 164.1, 169.3, 196.4.

Acknowledgements

This research is supported by the Iran National Science Foundation (INSF) (INSF 92013217) and the Islamic Azad University, Ayatollah Amoli Branch, Iran.

References and notes

- (a) R. Sersale, *Stud. Surf. Sci. Catal.* 1985, **24**, 503; (b) J. E. Naber and K.P. De Jong, *Stud. Surf. Sci. Catal.* 1994, **84**, 2197.
- D.W. Breck, *Zeolite Molecular Sieve Structure Chemistry and Use*, Wiley Interscience, New York, 1974.
- (a) N.V. Kumar and S.P. Rajendran, *Asian J. Chem.* 2004, **16**, 1911; (b) F. Hanawa, N. Fokialakis and A.L. Skaltsounis, *Planta Med.* 2004, **70**, 531; (c) Fujita, Y.; Oguri, H.; Oikawa, H. *J. Antibiot.* 2005, **58**, 425.
- C.L. Cantrell, K.K. Schrader, L.K. Mamonov, G.T. Sitpaeva, T.S. Kustova, C. Dunbar and D.E. Wedge, *J. Agric. Food Chem.* 2005, **53**, 7741.
- J.J. Chen, P.H. Chen, C.H. Liao, S.Y. Huang and I.S. Chen, *J. Nat. Prod.* 2007, **70**, 1444.
- X. Fan, D. Feng, Y. Qu, X. Zhang, J. Wang, P.M. Loiseau, G. Andrei, R. Snoeck and E.D. Clercq, *Bio. Med. Chem. Lett.* 2010, **20**, 809.
- I.S. Chen, I.W. Tsai, C.M. Teng, J.J. Chen, Y.L. Chang, F.N. Ko, M.C. Lu and J.M. Pezzuto, *Phytochemistry*, 1997, **46**, 525.
- C. Ito, M. Itoigawa, A. Furukawa, T. Hirano, T. Murata, N. Kaneda, Y. Hisada, K. Okuda and H. Furukawa, *J. Nat. Prod.* 2004, **67**, 1800.
- (a) K.D. McBrien, Q. Gao, S. Huang, S.E. Klohr, R.R. Wang and D. M. Pirmik, *J. Nat. Prod.* 1996, **59**, 1151; (b) C. Kamperdick, N.H. Van, T. Van Sung and G. Adam, *Phytochemistry* 1999, **50**, 177; (c) I.S. Chen, S.J. Wu, I.L. Tsai, T.S. Wu, J.M. Pezzuto, M.C. Lu, H. Chai, N. Suh and C.M. Teng, *J. Nat. Prod.* 1994, **57**, 1206.
- (a) D.R. da Rocha, A.C.G. de Souza, J.A.L.C. Resende, W. C. Santos, E.A. dos Santos, C. Pessoa, M.O. de Moraes, L.V. Costa-Lotufo, R.C. Montenegro and V.F. Ferreira, *Org. Biomol. Chem.* 2011, **9**, 4315; (b) Y. Dong, Q. Shi, K. Nakagawa-Goto, P.C. Wu, S.L. Morris-Natschke, A. Brossi, K.F. Bastow, J.Y. Lang, M.C. Hung and K.H. Lee, *Org. Biomol. Chem.* 2010, **18**, 803.
- S.B. Ferreira, F.d.C. da Silva, F.A.F.M. Bezerra, M.C.S. Lourenco, C.R. Kaiser, A.C. Pinto and V.F. Ferreira, *Arch. Pharm.* 2010, **343**, 81.

- M. He, N. Yang, C.L. Sun, X.J. Yao and M. Yang, *Med. Chem. Res.* 2011, **20**, 200.
- A. Shahrisa, M. Zirak, A.R. Mehdipour and R. Miri, *Chem. Heterocycl. Compd.* 2011, **46**, 1354.
- R. Schiller, L. Tichotova, J. Pavlik, V. Buchta, B. Melichar, I. Votruba, J. Kunes, M. Spulak, M. Pour, *Bioorg. Med. Chem. Lett.* 2010, **20**, 7358.
- H. Hussain, S. Aziz, B. Schulz and K. Krohn, *Nat. Prod. Commun.* 2011, **6**, 841.
- S. Osman, B.J. Albert, Y. Wang, M. Li, N.L. Czaicki and K. Koide, *Chem. Eur. J.* 2011, **17**, 895.
- S.S. Bisht, N. Jaiswal, A. Sharma, S. Fatima, R. Sharma, N. Rahuja, A.K. Srivastava, V. Bajpai, B. Kumar and R.P. Tripathi, *Carbohydr. Res.* 2011, **346**, 1191.
- S.M. Wang, G.W.A. Milne, X.J. Yan, I.J. Posey, M.C. Nicklaus, L. Graham, W.G. Rice, *J. Med. Chem.* 1996, **39**, 2047.
- W. Ying, S.Y. Mo, S.J. Wang, S. Li, Y.C. Yang and J.G. Shi, *Org. Lett.* 2005, **7**, 1675.
- (a) M.A. Nasser and S.M. Sadeghzadeh, *Monatsh. Chem.* 2013, **144**, 1551; (b) A. Hasaninejad, M. Shekouhy, N. Golzar, A. Zare and M.M. Doroodmand, *Appl. Catal. A*, 2011, **402**, 11; (c) P.P. Salvi, A.M. Mandhare, A.S. Sartape, D.K. Pawar, S.H. Han, S.S. Kolekar, *C. R. Chim.* 2011, **14**, 878; (d) M. Ghashang, S.S. Mansoor and K. Aswin, *Chin. J. Catal.* 2014, **35**, 127.
- (a) S.M. Baghbanian, N. Rezaei and H. Tashakkorian, *Green Chem.* 2013, **15**, 3446; (b) S.M. Baghbanian and M. Farhang, *J. Mol. Liq.* 2013, **183**, 45; (c) S.M. Baghbanian, Y. Babajani, H. Tashakkorian, S. Khaksar and M. Farhang, *C.R. Chim.* 2013, **16**, 129; (d) S.M. Baghbanian, M. Farhang and R. Baharfar, *Chin. Chem. Lett.* 2011, **22**, 555; (e) S.M. Baghbanian, S. Khaksar, S.M. Vahdat and M. Tajbakhsh, *Chin. Chem. Lett.* 2010, **2**, 563; (f) S.M. Baghbanian and M. Farhang, *RSC Adv.*, 2014, **4**, 11624; (g) S.M. Baghbanian and M. Farhang, *Syn. Comm.* 2014, **44**, 697; (h) S.M. Baghbanian and M. Farhang, *J. Iran. Chem. Soc.* 2013, **10**, 1033.
- S. Brunauer, L.S. Deming, W.E. Deming and E. Teller, *J. Am. Chem. Soc.* 1940, **62**, 1723.
- A. Radi, D. Pradhan, Y.K. Sohn and K.T. Leung, *ACS Nano* 2010, **4**, 1553.
- M. Tomellini, *J. Electron Spectrosc. Relat. Phenom.* 1992, **58**, 75.